

Supplementary Information

Enhancing Photocatalytic Hydrogen Evolution by Intramolecular Energy Transfer in Naphthalimide Conjugated Porphyrins

Govardhana Babu Bodedla,^{‡a} Lingling Li,^{‡a} Yuanyuan Che,^b Yijiao Jiang,^c Jun Huang,^d Jianzhang Zhao,^b Xunjin Zhu,^{*a}

^a Department of Chemistry and Institute of Advanced Materials, Hong Kong Baptist University, Waterloo Road, Kowloon Tong, Hong Kong, P. R. China. E-mail: xjzhu@hkbu.edu.hk.

^b School of Chemical Engineering and State Key Laboratory of Fine Chemicals, Dalian University of Technology, Dalian 116024, P. R. China.

^c School of Engineering, Macquarie University, Sydney, Australia.

^d School of Chemical and Biomolecular Engineering, The University of Sydney, Sydney, Australia.

‡ G.B.B and L. L. contribute equally to this work.

Kong. E-mail: xjzhu@hkbu.edu.hk

Experimental section

Figure S1. Optimized geometry (DFT; B3LYP) of the push-pull isomeric naphthalimide-porphyrins.

Figure S2. Frontier MOs of the push-pull isomeric naphthalimide-porphyrins.

Figure S3. (a) Differential pulse voltammograms of the porphyrins and (b) energy level alignment of the porphyrins.

Figure S4. Thermo gravimetric analysis of isomeric porphyrins.

Figure S5. The photocatalytic stability of the *para*-substituted isomer **ZnT(*p*-NI)PP** measured for 8 h.

Figure S6. Emission spectra of *para*-substituted isomer **ZnT(*p*-NI)PP** after loading the Pt cocatalyst.

Figure S7. ¹H NMR spectra of **3a** recorded in CDCl₃.

Figure S8. ¹³C NMR spectra of **3a** recorded in CDCl₃.

Figure S9. ¹H NMR spectra of **3b** recorded in CDCl₃.

Figure S10. ¹³C NMR spectra of **3b** recorded in CDCl₃.

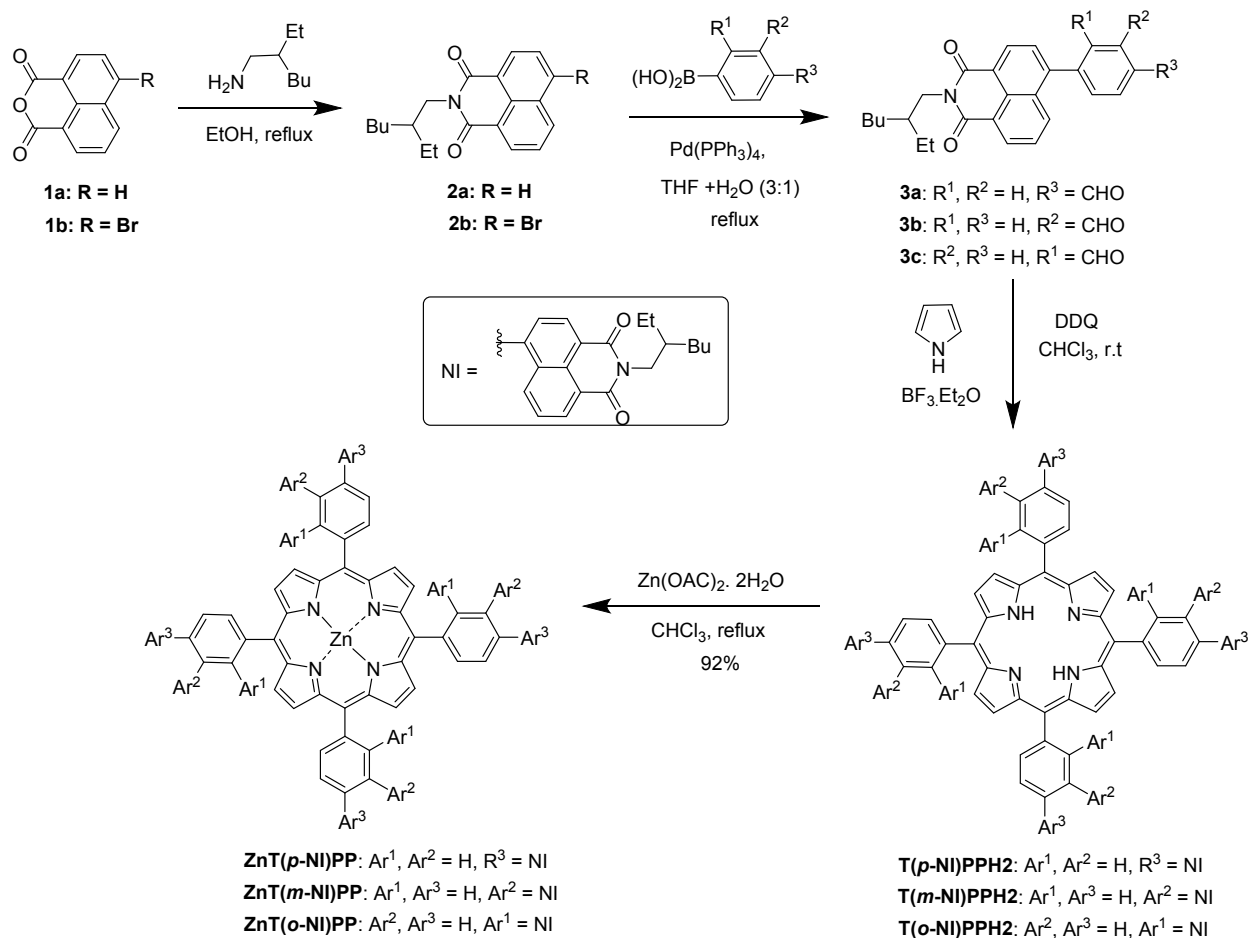
Figure S11. ¹H NMR spectra of **3c** recorded in CDCl₃.

Figure S12. ^{13}C NMR spectra of **3c** recorded in CDCl_3 .
Figure S13. ^1H NMR spectra of **T(*p*-NI)PPH2** recorded in CDCl_3 .
Figure S14. ^{13}C NMR spectra of **T(*p*-NI)PPH2** recorded in CDCl_3 .
Figure S15. ^1H NMR spectra of **T(*m*-NI)PPH2** recorded in CDCl_3 .
Figure S16. ^{13}C NMR spectra of **T(*m*-NI)PPH2** recorded in CDCl_3 .
Figure S17. ^1H NMR spectra of **T(*o*-NI)PPH2** recorded in CDCl_3 .
Figure S18. ^{13}C NMR spectra of **T(*o*-NI)PPH2** recorded in CDCl_3 .
Figure S19. ^1H NMR spectra of **ZnT(*p*-NI)PP** recorded in CDCl_3 .
Figure S20. ^{13}C NMR spectra of **ZnT(*p*-NI)PP** recorded in CDCl_3 .
Figure S21. ^1H NMR spectra of **ZnT(*m*-NI)PP** recorded in CDCl_3 .
Figure S22. ^{13}C NMR spectra of **ZnT(*m*-NI)PP** recorded in CDCl_3 .
Figure S23. ^1H NMR spectra of **ZnT(*o*-NI)PP** recorded in CDCl_3 .
Figure S24. ^{13}C NMR spectra of **ZnT(*o*-NI)PP** recorded in CDCl_3 .
Figure S25. MALDI-TOF-MS spectra of **ZnT(*p*-NI)PP**.
Figure S26. MALDI-TOF-MS spectra of **ZnT(*m*-NI)PP**.
Figure S27. MALDI-TOF-MS spectra of **ZnT(*o*-NI)PP**.

EXPERIMENTAL SECTION

Materials and Methods

All the chemicals used in this work were purchased from commercial sources and used as received. Solvents were dried by distilling over suitable dehydrating agents according to standard procedures. Purification of the compounds was performed by column chromatography with 100-200 mesh silica. ^1H and ^{13}C NMR spectra recorded in a NMR spectrometer operating at 400.00 and 100.00 MHz respectively. The chemical shifts were calibrated from the residual peaks observed for the deuterated solvent chloroform (CDCl_3) at δ 7.26 ppm for ^1H and δ 77.0 ppm for ^{13}C , respectively. High-resolution matrix-assisted laser desorption/ionization time-of-flight (MALDI-TOF) mass spectra were obtained with a Bruker Autoflex MALDI-TOF mass spectrometer. The optical absorption and emission spectra of the dyes were measured for the freshly prepared air equilibrated solutions at room temperature by using UV-Vis spectrophotometer spectrofluorimeter respectively. Thermogravimetric analyses were carried out under nitrogen atmosphere at heating a rate of 10 $^\circ\text{C}/\text{min}$. The cyclic voltammetry (CV) and differential pulse voltammetry (DPV) were recorded on an electrochemical workstation in tetrahydrofuran solution by using 0.1M tetrabutylammonium hexafluorophosphate (TBAPF_6) as supporting electrolyte. The experiments were performed at room temperature with a conventional three-electrode cell assembly consisting of a platinum wire as auxiliary electrode, a non-aqueous Ag/AgNO_3 reference electrode, ferrocene as internal standard and a glassy carbon working electrode.



Scheme S1. Synthesis of NI conjugated isomeric porphyrins

Fluorescence quantum yields (Φ_F)

The Φ_F of the porphyrins in degassed THF solution were calculated in by comparing with that of 5,10,15,20-tetraphenylporphyrin (**TPP**). **TPP** was used as fluorescence standard ($\lambda_{\text{exc}} = 552 \text{ nm}$) with $\Phi_F = 0.12$ in degassed toluene. The absorbance of the sample and reference solutions was measured by keeping at 0.1 and the emission of the sample and reference solutions was recorded at 552 nm excitation wavelength. The Φ_F was calculated according equation (Eq. 1):

$$\Phi_F^{\text{sample}} = \Phi_F^{\text{ref}} \left(\frac{S_{\text{sample}}}{S_{\text{ref}}} \right) \left(\frac{A_{\text{ref}}}{A_{\text{sample}}} \right) \left(\frac{n_{\text{sample}}}{n_{\text{ref}}} \right) \quad (1)$$

Where A_{ref} , S_{ref} , n_{ref} and A_{sample} , S_{sample} , n_{sample} represent the absorbance at the excited wavelength, integrated area under the fluorescence curves and the solvent refractive index of the standard and the sample solutions.

Preparation of photocatalytic systems

A 500 W xenon arc lamp (zhongjiaojinyuan, Model CEL-HXF300) was used as the trigger light source. The distance between the reactor and light source was 15 cm. The incident light radiation intensity was measured by a UV-A dual-channel radiation meter UV intensity meter (Beijing Normal University, Model FZ-A), and the average light intensity (15 cm away from the lamp, 15 Å) was ca. 80 mW/cm². The photocatalytic hydrogen (H₂) evolution experiments were performed in a quartz vial reactor (50 ml) sealed with a rubber septum, gas-closed system, at ambient temperature and pressure. Initially, the prepared sample powder (5 mg) was suspended in aqueous triethanolamine (TEOA) solution (Water: TEOA=9:1) under constant stirring. Then, 3 wt.% of Pt as co-catalyst was loaded by in situ photoreduction deposition method, H₂PtCl₆ aqueous as Pt source. The suspension was purged with nitrogen gas for 30 min to ensure anaerobic conditions and then it was placed at the position of 15 cm away from lamp. After 1h irradiation, the released gas (400 µL) was collected by syringe from the headspace of the reactor and was analyzed by gas chromatography (Shimadzu, GC-2014, Japan, with ultrapure Ar as a carrier gas) equipped with a TDX-01(5 Å molecular sieve column) and a thermal conductivity detector (TCD). Eventually, the total content of photocatalytic H₂ evolution was calculated according to the standard curve. Continuous stirring was applied to the whole process to keep the photocatalyst particles in suspension state and get the uniform irradiation.

The apparent quantum efficiency (AQE) was measured under the similar photocatalytic reaction conditions. Four low-power LEDs with monochromatic light (3 W, 365 nm) (Shenzhen

LAMPLIC Science Co. Ltd., China), which were placed 1cm away from the vial from four different directions, were applied as light sources. The focused intensity and illuminated areas for each LED were ca. 80.0 mW/cm² and 0.28 mm², respectively. QE was calculated via the following equation:

$$\text{AQE} = (2 \times \text{number of H}_2 \text{ molecules/number of incident photons}) \times 100\%.$$

The turnover number (TON) was calculated after 1 hours by using the following formula;

TON (turnover number) = moles of H₂ molecules evolved / moles of active sites (platinum on the photocatalyst).

The turnover frequency (TOF) = TON/t(h)

Photoelectrochemical Measurement

Photoelectrochemical tests were performed on a three-electrode system using an electrochemical workstation (CHI660C Instruments, China) with Pt wire (counter electrode) and saturated calomel electrode (SCE, reference electrode). The working electrode was fluorine-doped tin oxide (FTO) glass coated with a sample film on the conductive surface. Typically, 2 mg of sample were dissolved in 1 mL of dichloromethane (DCM), and then applied on the conductive surface of FTO glass using drop dispense method. The light source was an LED monochromatic point lamp (3 W, 365 nm). The light spot effective area on the working electrode was set as 28.26 mm². 8 mL volume of 0.5 M Na₂SO₄ aqueous solution acted as the electrolyte. The open-circuit voltages were set as the initial bias voltages in the transient photocurrent responses tests. The electrochemical impedance spectroscopy (EIS) was recorded over a frequency range of 1-10⁵ Hz with an amplitude of 5.0 mV.

Theoretical calculations

In order to further understand the electronic structure of the isomeric NI-porphyrins, we have performed density functional theoretical (DFT) calculations using Gaussian 09W program.

The ground state geometry of the porphyrins (ethylhexyl groups were replaced with methyl unit) was optimized at the B3LYP/Genecp/ /LANL2DZ level. The optimized geometry of the isomeric NI-porphyrins is shown in **Figure S1**. The computed frontier molecular orbitals HOMO, HOMO-1, LUMO and LUMO+1 of the porphyrins are shown in **Figure S2**. The vertical excitation energies, their oscillator strengths and orbital contribution are listed in **Table S1**. From the angles between average planes of the NI groups and the porphyrin ring, we noticed two important points: (i) the NI groups around the porphyrin ring are not symmetric to each other and (ii) the distance between the NI plane and porphyrin ring plane are not same in all the porphyrins. More importantly, in the *para*-substituted isomer **ZnT(*p*-NI)PP**, the angles between the NI plane and the porphyrin ring plane are lies in the range of 8.74-11.02 °A which are very less compared to the angles between the NI plane and the porphyrin ring plane of other isomers **ZnT(*p*-NI)PP** and **ZnT(*p*-NI)PP**. The less angles between the NI plane and the porphyrin ring indicating that, the distance between the NI groups and the porphyrin ring is less spatially in the *para*-substituted isomer **ZnT(*p*-NI)PP**. According to the Dexter energy transfer mechanism, the energy transfer between the energy donor and the energy acceptor occurs if the donor and acceptor proximity close in the range of 6-20 °A.¹ Based on this, the presence of Dexter energy transfer allowed distance between the NI groups and the porphyrin ring in the *para*-substituted isomer **ZnT(*p*-NI)PP** could also exhibits the efficient energy transfer between the NI energy donor and energy the porphyrin acceptor. Also, this is well matched to the experimentally observed high energy transfer efficiency for the *para* isomer compared to other isomers.

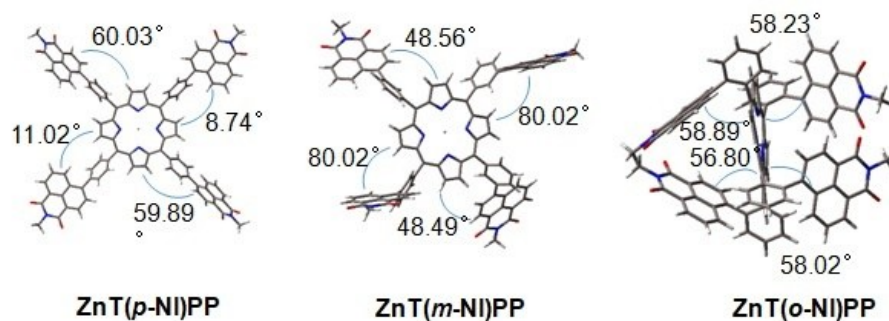


Figure S1. Optimized geometry (DFT; B3LYP) of the push-pull isomeric naphthalimide-porphyrins. Only one enantiomer for each compound is shown for simplicity. The angles are those formed by the average planes between the porphyrin and naphthalimide.

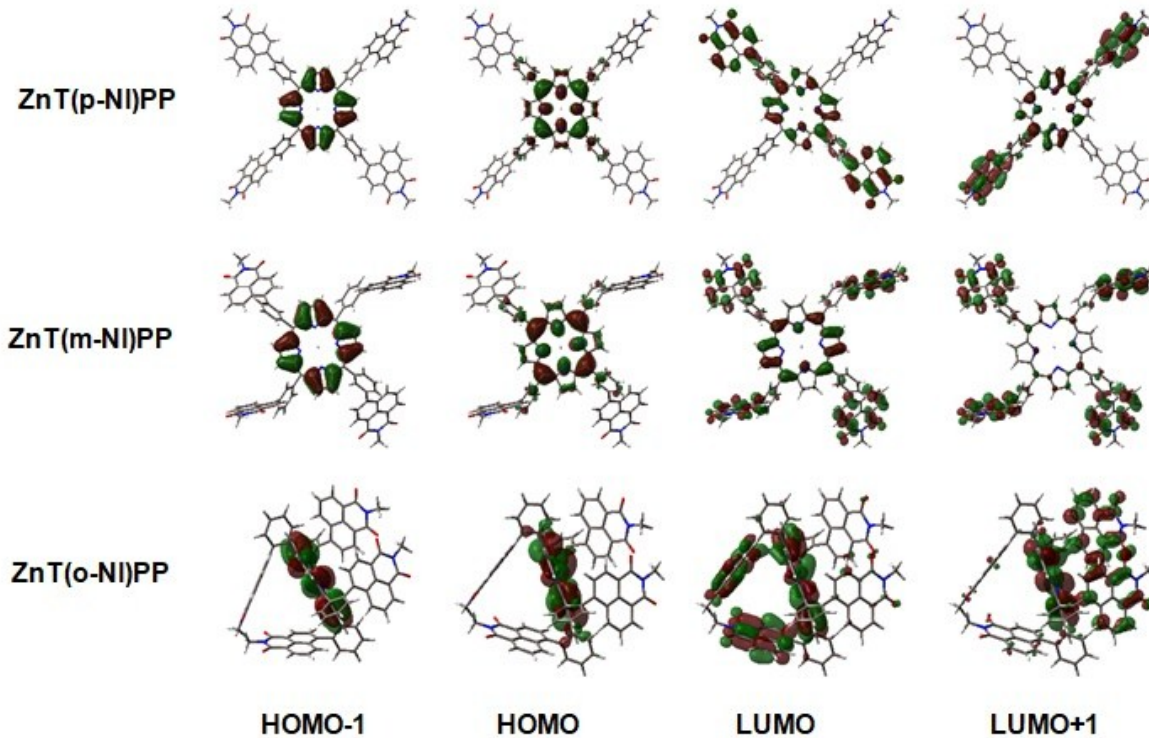


Figure S2. Frontier MOs of the push-pull isomeric naphthalimide-porphyrins. THF was used as solvent in the calculations (CPCM model). The calculations are at the B3LYP/Genecp//LANL2DZ level using Gaussian 09W.

Table S1. Lowest-lying Vertical (at S_0 Geometry) Doublet Electronic Transition Energies (eV / nm) and Oscillator Strengths (in Parentheses) of compound. Calculated by TDDFT//B3LYP/LANL2DZ, based on the DFT//B3LYP/LANL2DZ Optimized Ground State Geometries. THF was used as solvent in the calculations (CPCM model).

TDDFT/B3LYP					
	Electronic transition	Energy [eV/nm] ^a	f^b	Major contributors (%) Composition ^c	μ_g (D)
ZnT(<i>p</i>-NI)PP	$S_0 \rightarrow S_1$	2.21 / 561	0.1483	H→L	1.0626
	$S_0 \rightarrow S_6$	2.45 / 506	0.1129	H→L+5	
	$S_0 \rightarrow S_{11}$	3.02 / 411	2.4192	H-1→L+5	
	$S_0 \rightarrow S_{12}$	3.02 / 410	2.2717	H-1→L+4	
	$S_0 \rightarrow S_{15}$	3.38 / 367	0.2960	H-3→L	
	$S_0 \rightarrow S_{16}$	3.39 / 366	0.3211	H-3→L+1	
ZnT(<i>m</i>-NI)PP	$S_0 \rightarrow S_1$	2.23 / 555	0.0672	H→L	0.8426
	$S_0 \rightarrow S_7$	2.67 / 464	0.0990	H-1→L	
	$S_0 \rightarrow S_{11}$	3.03 / 409	2.2023	H-1→L+4	
	$S_0 \rightarrow S_{13}$	3.37 / 368	0.8288	H-2→L	
	$S_0 \rightarrow S_{14}$	3.40 / 365	0.1943	H-3→L	
ZnT(<i>o</i>-NI)PP	$S_0 \rightarrow S_1$	2.20 / 564	0.0181	H→L	0.5324
	$S_0 \rightarrow S_3$	2.36 / 524	0.0221	H→L+2	
	$S_0 \rightarrow S_8$	2.57 / 482	0.0310	H-1→L+3	
	$S_0 \rightarrow S_9$	2.58 / 481	0.0235	H-1→L+4	
	$S_0 \rightarrow S_{11}$	3.01 / 412	0.9248	H-1→L+4	
	$S_0 \rightarrow S_{12}$	3.02 / 411	0.9392	H-1→L+5	

$S_0 \rightarrow S_{21}$	3.47 / 357	0.2980	H-2 \rightarrow L+2
$S_0 \rightarrow S_{22}$	3.49 / 355	0.2152	H-3 \rightarrow L+3
$S_0 \rightarrow S_{23}$	3.52 / 352	0.3534	H-4 \rightarrow L+3

^a Only the selected low-lying excited states are presented. ^b Oscillator strengths. ^c Only the main configurations are presented. ^d The CI coefficients are in absolute values

Synthesis

The naphthalimide intermediates, 2-(2-ethylhexyl)-1*H*-benzo[de]isoquinoline-1,3(2*H*)-dione (**2a**) and 6-bromo-2-(2-ethylhexyl)-1*H*-benzo[de]isoquinoline-1,3(2*H*)-dione (**2b**), and **ZnTPP** were synthesized according to the literature procedures and characterized by comparing their ¹H NMR spectra with those found in the literature.²⁻⁴

4-(2-(2-Ethylbutyl)-1,3-dioxo-2,3-dihydro-1*H*-benzo[de]isoquinolin-6-yl)benzaldehyde (3a):

In a 100 mL two-neck round-bottom flask, 6-bromo-2-(2-ethylhexyl)-1*H*-benzo[de]isoquinoline-1,3(2*H*)-dione, **2** (0.5 g, 1.28 mmol), 4-formylphenylboronic acid (0.23 g, 1.54 mmol), potassium carbonate (0.53 g, 3.84 mmol) and 30 mL THF/H₂O (3:1, v/v) were taken and purged with nitrogen. After addition of Pd(PPh₃)₄ (50 mg, 2 mol %) the reaction mixture was refluxed for 24 h. After completion of reaction, it was diluted with dichloromethane and water. The organic layer was separated, dried over Na₂SO₄ and solvent removed under reduced pressure. The resulted crude reaction mixture containing product was purified by column chromatography with silica using dichloromethane/hexane (1:1, v/v) as eluent. Off-white solid; yield 0.5 g, 94.0%; ¹H NMR (CDCl₃, 400.00 MHz) δ 0.87-0.91 (m, 3 H), 0.95 (t, J = 7.2 Hz, 3 H), 1.26-1.44 (m, 8 H), 1.96-1.99 (m, 1 H), 4.14-4.18 (m, 2 H), 7.69-7.76 (m, 4 H), 8.08 (dd, J = 6.4 Hz, 1.6 Hz, 2 H), 8.18 (dd, J = 8.6 Hz, 1.2 Hz, 1 H), 8.65-8.69 (m, 2 H), 10.16 (s, 1 H). ¹³C NMR (CDCl₃, 100.00 MHz) δ 10.66, 14.10, 23.05, 24.05, 28.67, 30.73, 37.89, 44.14, 122.52, 123.01, 127.26, 127.84, 128.57, 129.60, 129.93, 130.63, 131.32, 131.78, 136.11, 144.89, 144.97, 164.11, 164.31, 191.56.

3-(2-(2-Ethylbutyl)-1,3-dioxo-2,3-dihydro-1H-benzo[de]isoquinolin-6-yl)benzaldehyde (3b):

It was synthesized by following the procedure described above for **3a**, except using of 3-formylphenylboronic acid instead of 4-formylphenylboronic acid; Light yellow solid; yield 94.2%; ¹H NMR (CDCl₃, 400.00 MHz) δ 0.87-0.96 (m, 6 H), 1.31-1.43 (m, 8 H), 1.94-2.00 (m, 2 H), 4.10-4.20 (m, 2H), 7.72-7.80 (m, 4 H), 8.03 (d, *J* = 1.6 Hz, 1 H), 8.05-8.06 (m, 1 H), 8.16 (dd, *J* = 8.4 Hz, 1.2 Hz, 1 H), 8.644-8.68 (m, 2 H), 10.14 (s, 1 H). ¹³C NMR (CDCl₃, 100.00 MHz) δ 10.65, 14.12, 23.05, 24.02, 28.64, 30.70, 37.84, 44.06, 122.26, 122.91, 127.17, 127.93, 128.47, 129.46, 129.63, 129.72, 130.61, 131.19, 131.67, 135.60, 136.72, 139.70, 144.81, 164.00, 164.19, 191.61.

2-(2-(2-Ethylbutyl)-1,3-dioxo-2,3-dihydro-1H-benzo[de]isoquinolin-6-yl)benzaldehyde (3c):

It was synthesized by following the procedure described above for **3a**, except using of 2-formylphenylboronic acid instead of 4-formylphenylboronic acid; Off-white solid; yield 96.0%; ¹H NMR (CDCl₃, 400.00 MHz) δ 0.87-0.97 (m, 6 H), 1.27-1.45 (m, 8 H), 1.95-2.01 (m, 1 H), 4.11-4.22 (m, 2 H), 7.45 (dd, *J* = 7.6 Hz, 0.8 Hz, 1 H), 7.67-7.71 (m, 3 H), 7.75-7.79 (m, 1 H), 7.82-7.85 (m, 1 H), 8.14 (dd, *J* = 8.0 Hz, 1.2 Hz, 1 H), 8.64 (dd, *J* = 7.2 Hz, 0.8 Hz, 1 H), 8.68 (d, *J* = 7.2 Hz, 1 H), 9.68 (s, 1 H). ¹³C NMR (CDCl₃, 100.00 MHz) δ 10.68, 14.13, 23.10, 24.06, 28.70, 30.76, 37.96, 44.22, 122.84, 123.07, 127.55, 128.23, 128.58, 128.76, 129.26, 130.34, 131.16, 131.40, 131.45, 131.85, 133.90, 134.63, 141.57, 142.53, 164.20, 164.38, 190.76.

T(*p*-NI)PPH2:

In a 250 mL two-neck round-bottom flask 4-(2-(2-ethylbutyl)-1,3-dioxo-2,3-dihydro-1H-benzo[de]isoquinolin-6-yl)benzaldehyde, **3a** (1.0 g, 2.4 mmol), pyrrole (180 μL, 2.64 mmol) and chloroform (100 mL) were taken and purged with nitrogen for 20 min. After BF₃-Et₂O (400 μL) was added and the reaction mixture was stirred for 6 h at room temperature under nitrogen and

dark. After 2,3-dichloro-5,6-dicyanobenzoquinone (DDQ) (1.2 g, 5.3 mmol) was added, and the reaction mixture was stirred for 30 min. The reaction was quenched by the addition of triethylamine (5 mL). After completion of reaction, the solvent was removed and the resulted crude product was purified by column chromatography with silica using dichloromethane/hexane (1:1, v/v) as eluent. Dark-red color solid: yield 1.1 g, 25.0%. ^1H NMR (CDCl_3 , 400.00 MHz) δ – 2.59 (s, 2 H), 0.93 (t, $J = 6.8$ Hz, 12 H), 0.10 (t, d, $J = 7.2$ Hz, 12 H), 1.36-1.50 (m, 32 H), 2.01-2.08 (m, 4 H), 4.17-4.28 (m, 8 H), 7.89-7.99 (m, 12 H), 8.11 (d, $J = 7.6$ Hz, 4 H), 8.49 (d, $J = 8.0$ Hz, 8 H), 8.71-8.77 (m, 8 H), 8.84 (d, $J = 7.2$ Hz, 4 H), 9.11 (s, 8 H). ^{13}C NMR (CDCl_3 , 100.00 MHz) δ 10.70, 14.14, 23.11, 24.09, 28.74, 30.78, 37.97, 44.24, 119.73, 122.10, 123.10, 127.08, 128.21, 128.40, 128.85, 130.05, 130.94, 131.35, 132.38, 134.93, 138.40, 142.24, 146.20, 164.45, 164.60.

T(*m*-NI)PPH2:

It was synthesized by following the procedure described above for **T(*p*-NI)PPH2**, except using of **3b** instead of **3a**. Wine-red color solid: yield 23.0%; ^1H NMR (CDCl_3 , 400.00 MHz) δ – 2.73 (s, 2 H), 0.86-0.94 (m, 24 H), 1.30-1.39 (m, 32 H), 1.95 (m, 4 H), 4.09-4.18 (m, 8 H), 7.73-7.84 (m, 4 H), 7.97-8.05 (m, 12 H), 8.39-8.40 (m, 8 H), 8.61-8.73 (m, 12 H), 9.04 (s, 8 H). ^{13}C NMR (CDCl_3 , 100.00 MHz) δ 10.62, 14.07, 23.02, 24.00, 28.65, 30.69, 37.85, 44.12, 119.62, 122.02, 122.99, 127.06, 127.11, 128.27, 128.71, 129.48, 130.03, 130.06, 130.09, 130.79, 131.22, 132.12, 132.18, 132.25, 134.46, 135.72, 135.79, 135.87, 137.40, 142.49, 146.02, 146.08, 146.15, 164.24, 164.29, 164.33, 164.41, 164.46, 164.51.

T(*o*-NI)PPH2: It was synthesized by following the procedure described above for **T(*p*-NI)PPH2**, except using of **3c** instead of **3a**. Wine-red color solid: yield 28.0%; ^1H NMR (CDCl_3 , 400.00 MHz) δ : The splitting of NMR signals was not observed due to highly steric hindered

structure. ^{13}C NMR (CDCl_3 , 100.00 MHz) δ 10.23, 10.32, 10.43, 13.98, 14.03, 22.79, 22.84, 22.94, 23.00, 23.56, 23.71, 23.77, 28.29, 28.42, 28.51, 30.28, 30.46, 30.58, 37.03, 37.11, 37.44, 37.60, 43.69, 43.86, 44.09, 117.31, 117.75, 118.19, 120.64, 120.74, 120.81, 120.96, 122.24, 122.39, 122.45, 122.53, 126.11, 126.32, 126.45, 126.60, 126.71, 127.57, 127.66, 127.75, 127.83, 127.94, 128.04, 128.12, 128.17, 128.34, 128.89, 129.41, 129.49, 129.96, 130.08, 130.17, 130.25, 130.44, 130.62, 130.74, 130.85, 130.89, 132.18, 132.43, 132.61, 140.56, 140.60, 140.78, 140.83, 140.87, 140.92, 140.99, 141.04, 141.88, 145.02, 145.14, 162.57, 163.08, 163.52, 163.55, 164.17, 164.22.

ZnT(*p*-NI)PP:

A mixture of **T(*p*-NI)PPH2** (0.20 g, 0.11 mmol), $\text{Zn}(\text{OAc})_2 \cdot 2\text{H}_2\text{O}$ (0.25 g, 1.1 mmol) and CHCl_3 (10 mL) was refluxed overnight. After completion of the reaction, solvent was removed and the resulted crude product was purified by column chromatography with silica using dichloromethane as eluent. Dark-red color solid: yield 0.18 g, 92.0%. ^1H NMR (CDCl_3 , 400.00 MHz) δ 0.90-0.99 (m, 24 H), 1.35-1.46 (m, 32 H), 1.99-2.04 (m, 4 H), 4.10 (m, 4.20), 7.89-7.93 (m, 4 H), 7.97 (d, $J = 8.4$ Hz, 8 H), 8.11 (d, $J = 7.2$ Hz, 4 H), 8.48 (d, $J = 8.0$ Hz, 8 H), 8.70-8.75 (m, 8 H), 8.78 (d, $J = 7.7$ Hz, 4 H), 9.20 (s, 1 H). ^{13}C NMR (CDCl_3 , 100.00 MHz) δ 10.46, 14.07, 23.02, 23.77, 28.54, 30.53, 37.67, 43.71, 120.47, 121.54, 122.65, 126.93, 128.15, 128.53, 129.86, 130.82, 131.19, 132.18, 132.31, 134.90, 137.90, 143.17, 146.24, 150.16, 164.10, 164.23. HRMS (ESI): m/z Calcd for $\text{C}_{124}\text{H}_{112}\text{N}_8\text{O}_8\text{Zn}$: 1906.7918 $[\text{M}]^+$; found: 1906.7771.

ZnT(*m*-NI)PP:

It was synthesized by following the procedure described above for **ZnT(*p*-NI)PP**, except using of **T(*m*-NI)PPH2** instead of **T(*p*-NI)PPH2**. Wine-red color solid: yield 90.0%; ^1H NMR (CDCl_3 , 400.00 MHz) δ 0.68-0.82 (m, 24 H), 1.18-1.20 (m, 32 H), 1.71 (s, 4 H), 3.55-3.73 (m, 8 H), 7.63-

7.71 (m, 4 H), 7.76-7.94 (m, 12 H), 8.13-8.39 (m, 16 H), 8.50-8.61 (m, 4 H), 9.05 (d, $J = 5.6$ Hz, 8 H). ^{13}C NMR (CDCl_3 , 100.00 MHz) δ 10.27, 13.96, 22.90, 23.56, 28.42, 30.38, 37.51, 43.53, 120.23, 121.14, 121.27, 122.39, 122.48, 126.77, 126.86, 128.03, 128.16, 128.24, 128.31, 128.98, 129.69, 129.80, 130.57, 131.10, 132.03, 132.15, 134.24, 135.36, 135.43, 135.54, 135.73, 136.91, 143.47, 143.54, 146.05, 146.13, 146.18, 150.06, 163.70, 163.82, 163.90, 163.96, 164.05. HRMS (ESI): m/z Calcd for $\text{C}_{124}\text{H}_{112}\text{N}_8\text{O}_8\text{Zn}$: 1906.7918 $[\text{M}]^+$; found: 1906.7953.

ZnT(*o*-NI)PP:

It was synthesized by following the procedure described above for **ZnT(*p*-NI)PP**, except using of **T(*o*-NI)PPH2** instead of **T(*p*-NI)PPH2**. Wine-red color solid: yield 95.0%; ^1H NMR (CDCl_3 , 400.00 MHz) δ : The splitting of NMR signals was not observed due to highly steric hindered structure. ^{13}C NMR (CDCl_3 , 100.00 MHz) δ : 10.22, 10.33, 10.39, 10.51, 13.96, 22.84, 22.93, 22.98, 23.59, 23.74, 28.33, 28.46, 30.30, 30.47, 37.21, 37.43, 37.52, 37.60, 43.71, 43.87, 44.04, 118.13, 111.33, 118.58, 118.76, 119.0, 120.16, 120.68, 122.09, 122.38, 125.99, 126.33, 126.61, 127.61, 127.80, 128.06, 128.63, 128.79, 128.97, 129.29, 130.03, 130.19, 130.44, 130.76, 131.22, 131.55, 132.08, 132.23, 132.61, 132.78, 134.47, 134.92, 135.18, 135.75, 136.10, 140.22, 140.42, 140.59, 141.42, 141.59, 141.64, 141.70, 141.81, 142.05, 144.49, 145.32, 145.43, 145.69, 145.80, 148.69, 148.94, 149.11, 149.23, 149.44, 149.77, 149.96, 150.06, 150.23, 150.54, 163.68, 164.21, 164.27. HRMS (ESI): m/z Calcd for $\text{C}_{124}\text{H}_{112}\text{N}_8\text{O}_8\text{Zn}$: 1907.79964 $[\text{M}+1]$; found: 1907.8041.

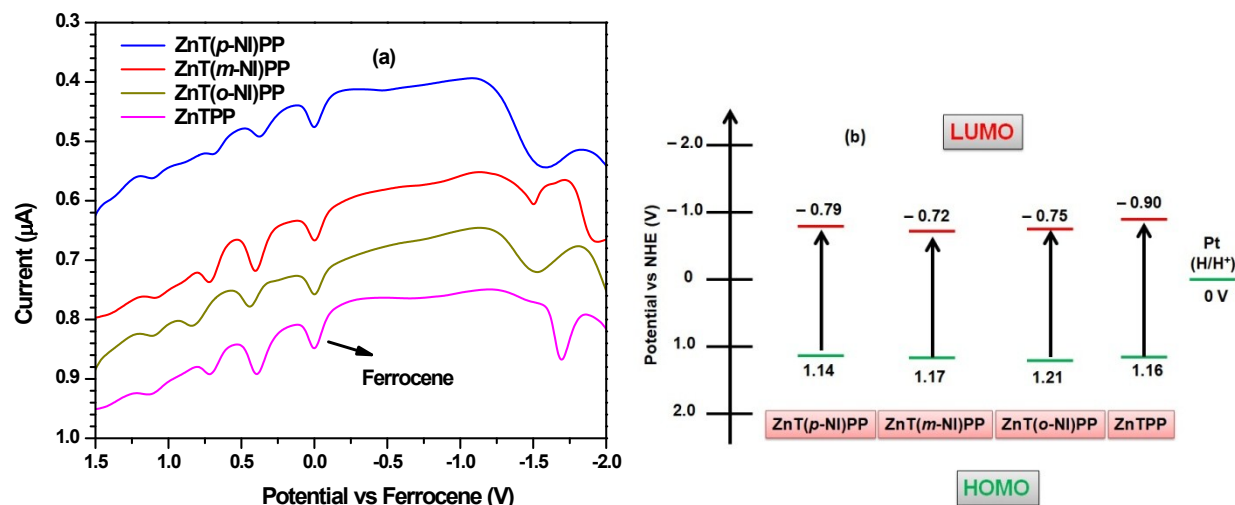


Figure S3. (a) Differential pulse voltammograms of the porphyrins and (b) energy level alignment of the porphyrins.

Thermal Properties

The thermal stability of the porphyrins was measured by thermogravimetric analysis (TGA), under a flow of nitrogen atmosphere at the heating rate of 10 °C/min. Thermal onset decomposition temperatures (T_{onset}) values of the dyes are listed in Table 2. The T_{onset} values of the porphyrins are in the order: **ZnTPP** (257) < **ZnT(o-NI)PP** (444) < **ZnT(m-NI)PP** (452) < **ZnT(p-NI)PP** (465). This indicates that the porphyrins such as **ZnT(o-NI)PP**, **ZnT(m-NI)PP**, **ZnT(p-NI)PP** featuring NI possessing high thermal stability than the NI free porphyrin, **ZnTPP**. Also, it is interesting to observe that when swiping the NI moiety from *ortho*- to *para*-position on the phenyl linker attached to the porphyrin unit increasing the thermal stability from 445 to 465. All these results indicating that the introduction and position of NI on the porphyrin ring plays an important role to achieve high thermal stability of isomeric NI-porphyrins.

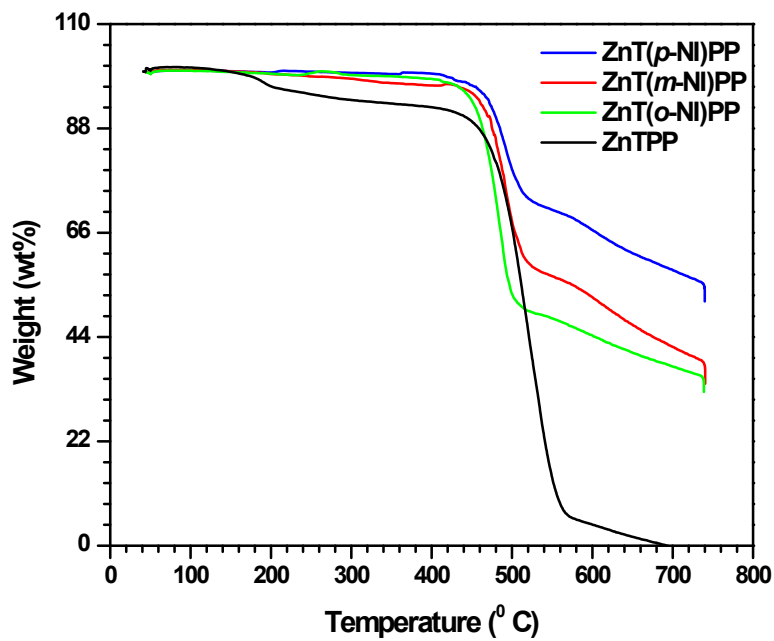


Figure S4. Thermo gravimetric analysis of isomeric porphyrins.

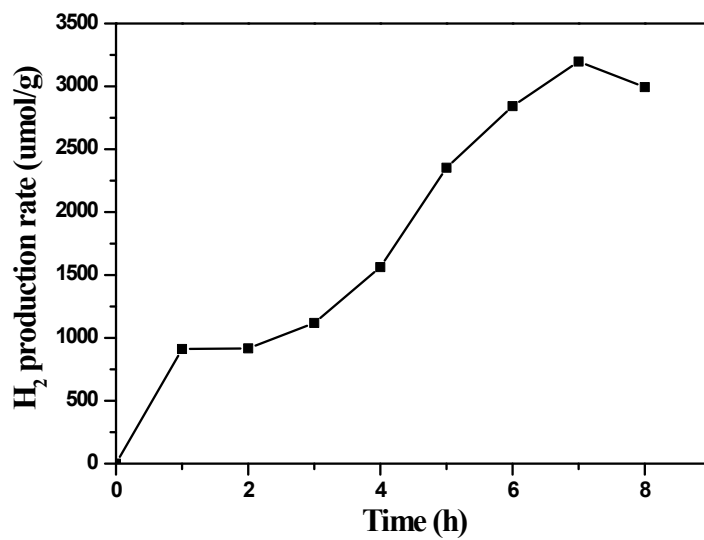


Figure S5. The photocatalytic stability of the *para*-substituted isomer ZnT(*p*-NI)PP measured for 8 h.

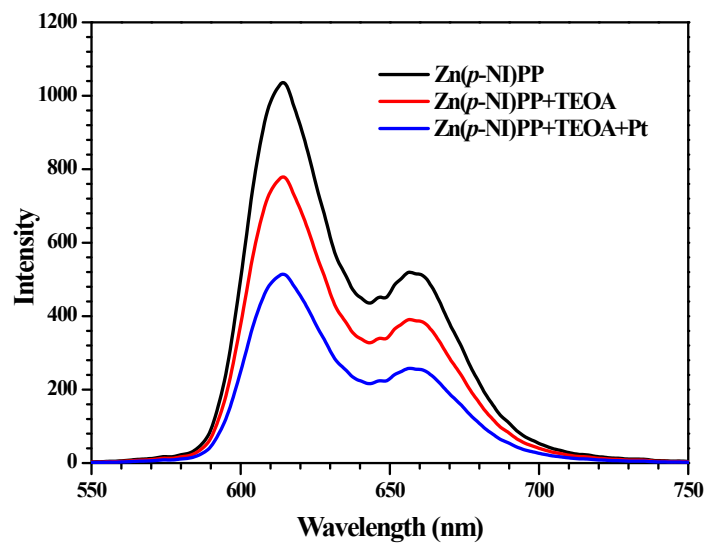


Figure S6. Emission spectra of the isomeric porphyrins after loading the Pt cocatalyst.

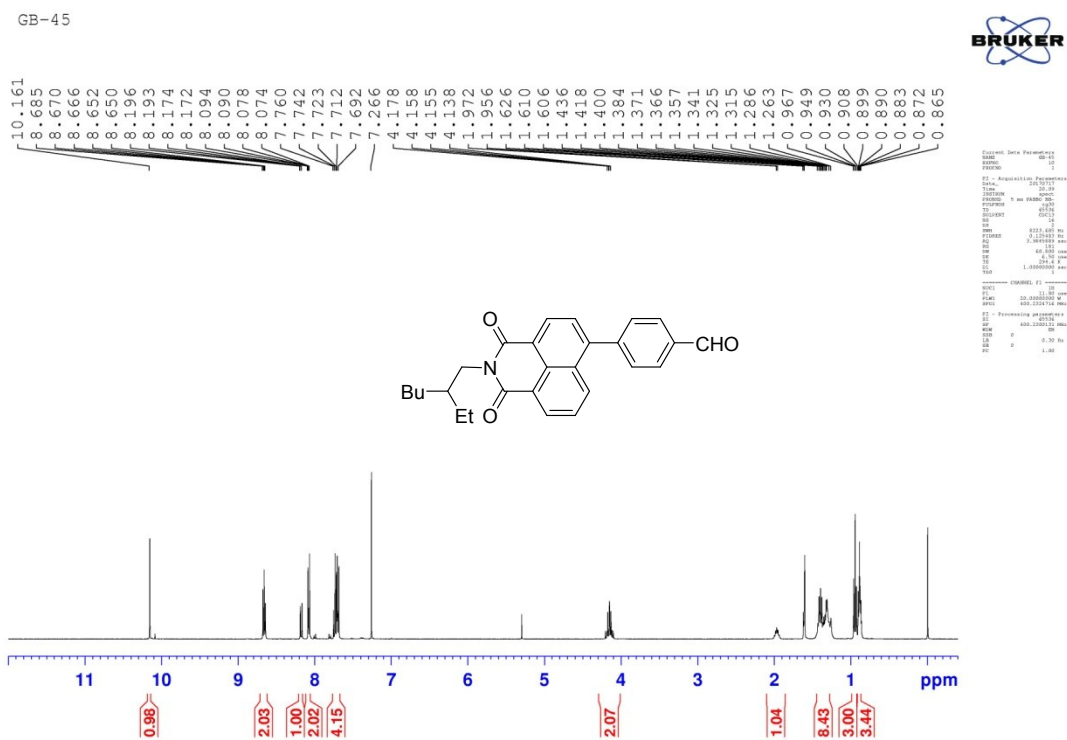


Figure S7. ¹H NMR spectra of **3a** recorded in CDCl₃.

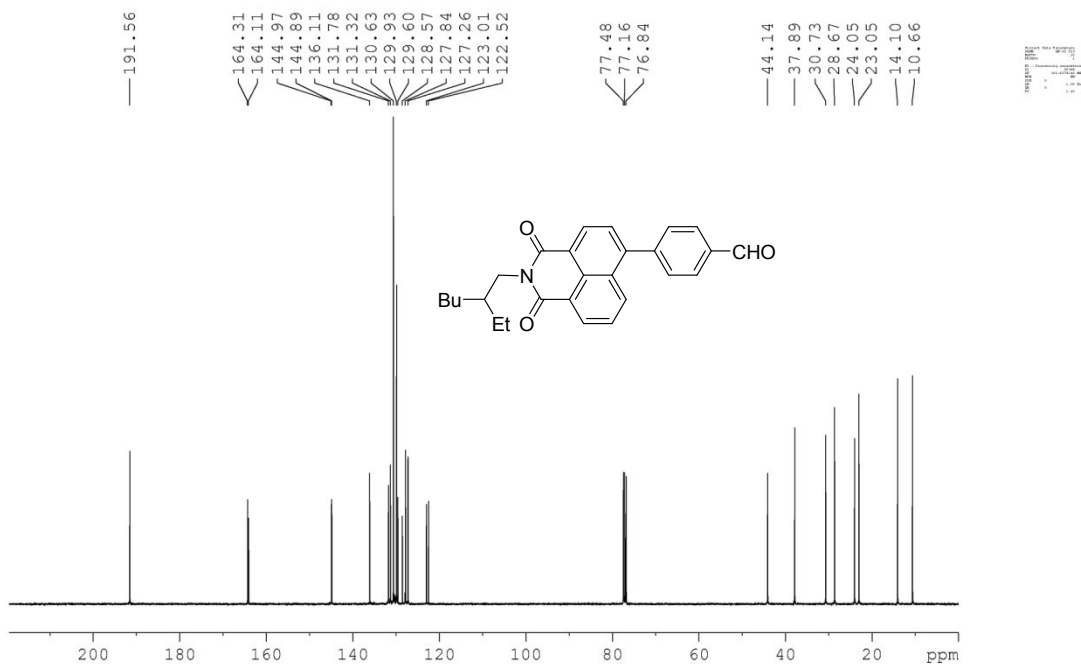


Figure S8. ¹³C NMR spectra of **3a** recorded in CDCl₃.

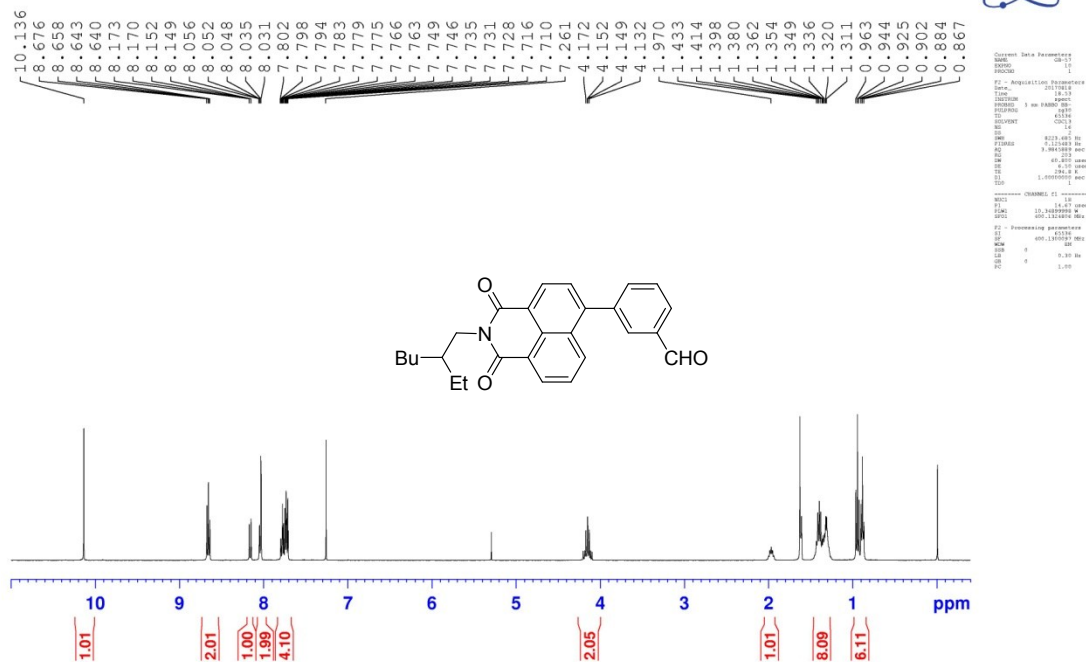


Figure S9. ¹H NMR spectra of **3b** recorded in CDCl₃.

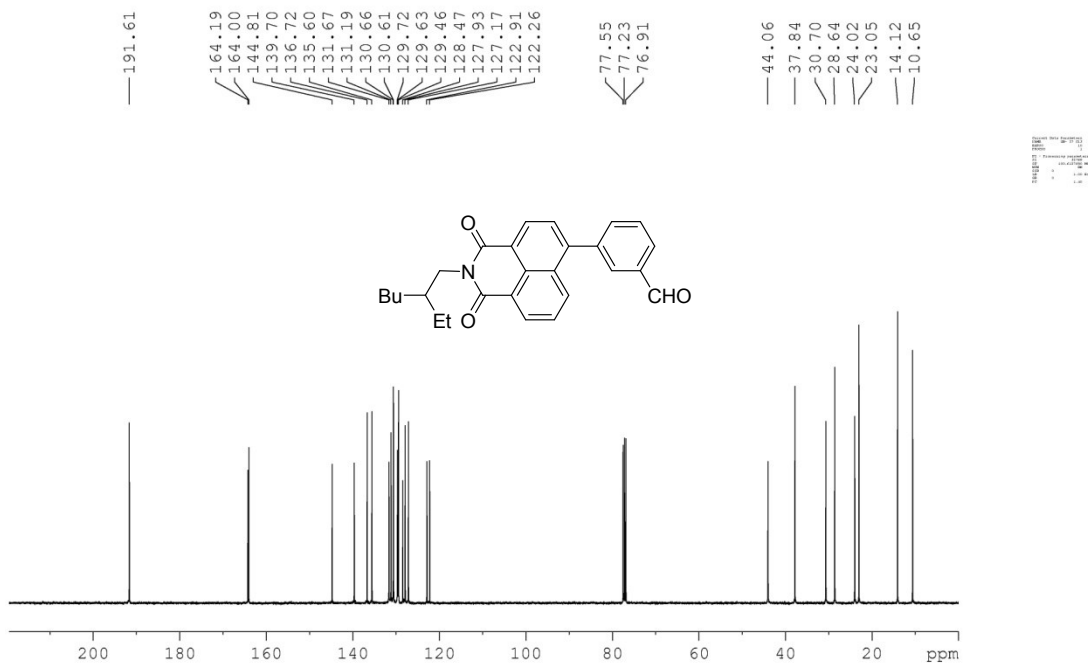


Figure S10. ¹³C NMR spectra of **3b** recorded in CDCl₃.

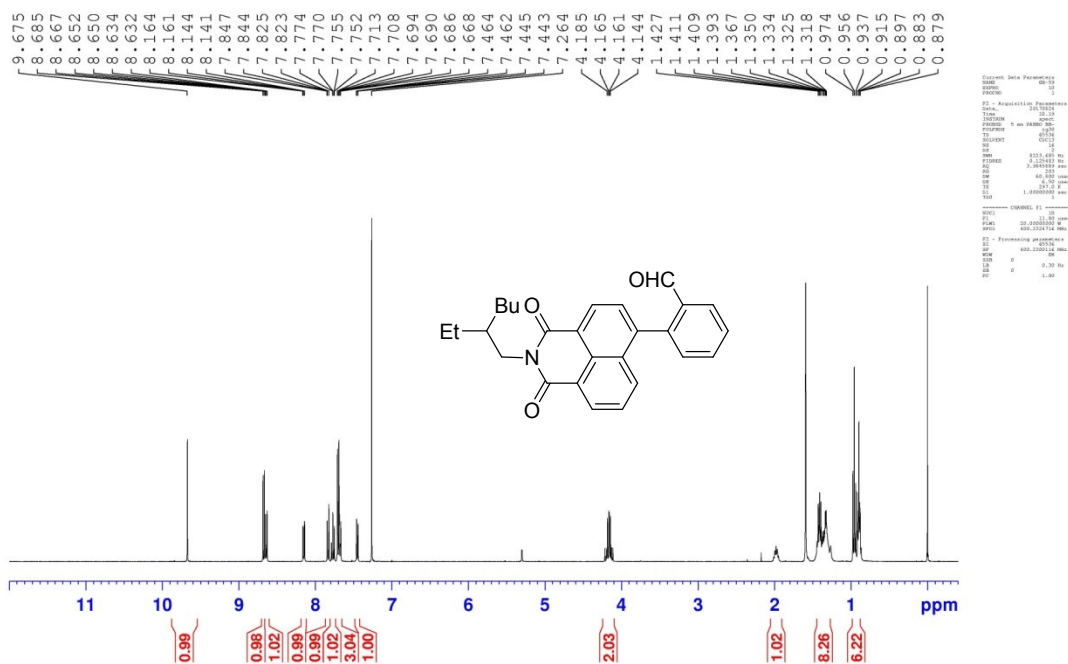


Figure S11. ¹H NMR spectra of **3c** recorded in CDCl₃.

GB-59

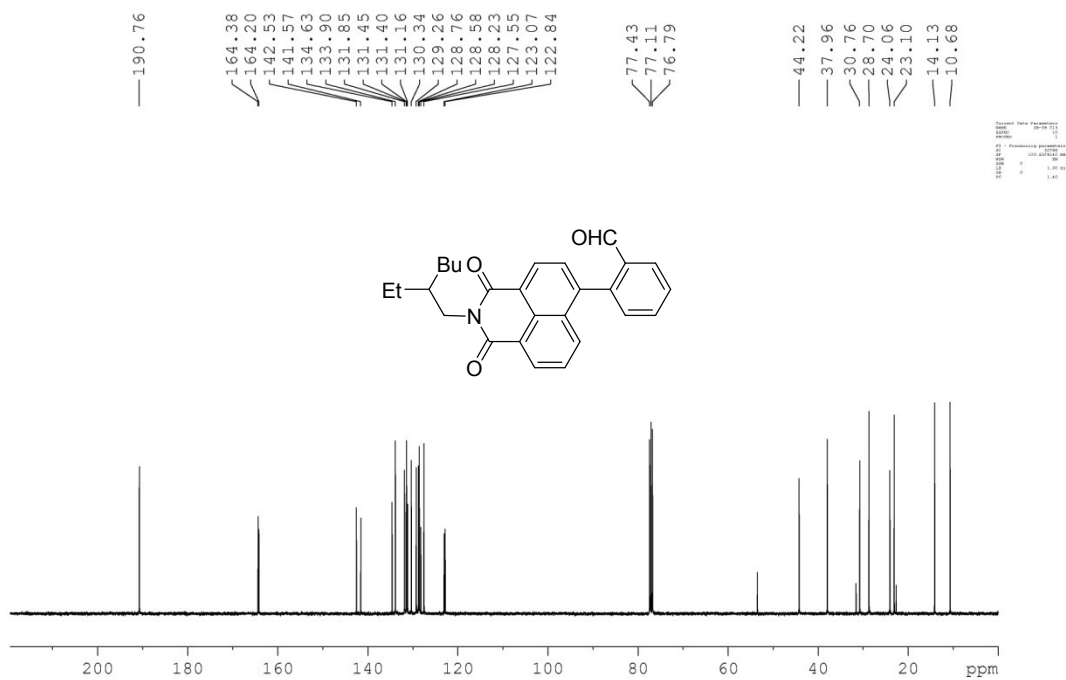


Figure S12. ^{13}C NMR spectra of **3c** recorded in CDCl_3 .

GB-48

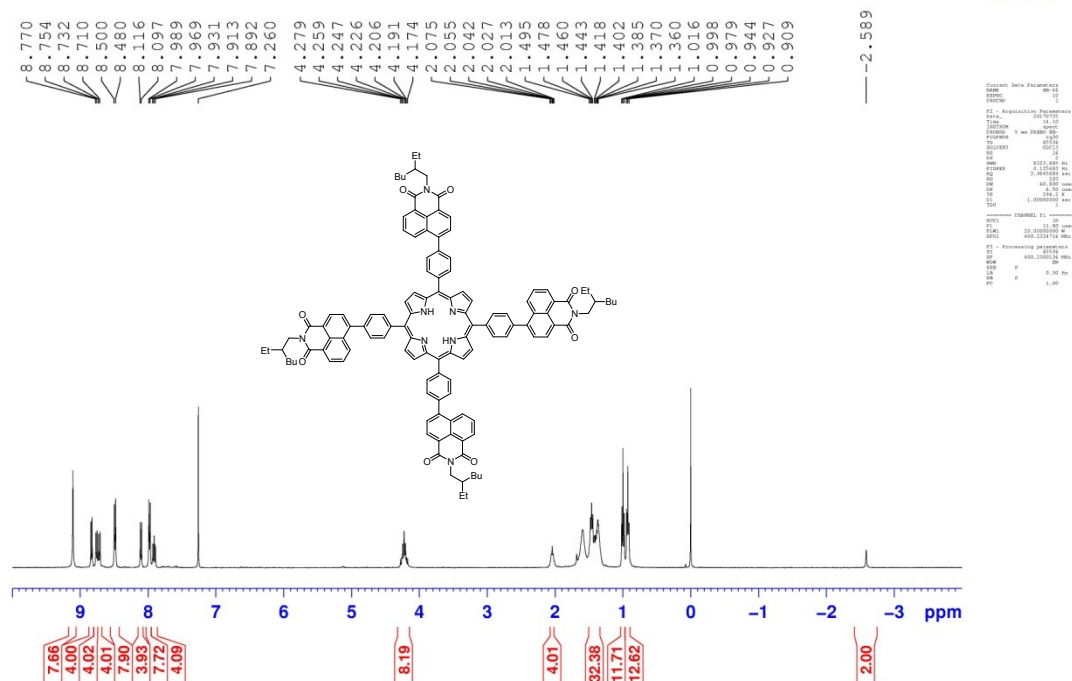


Figure S13. ^1H NMR spectra of **T(p-NI)PPH2** recorded in CDCl_3 .

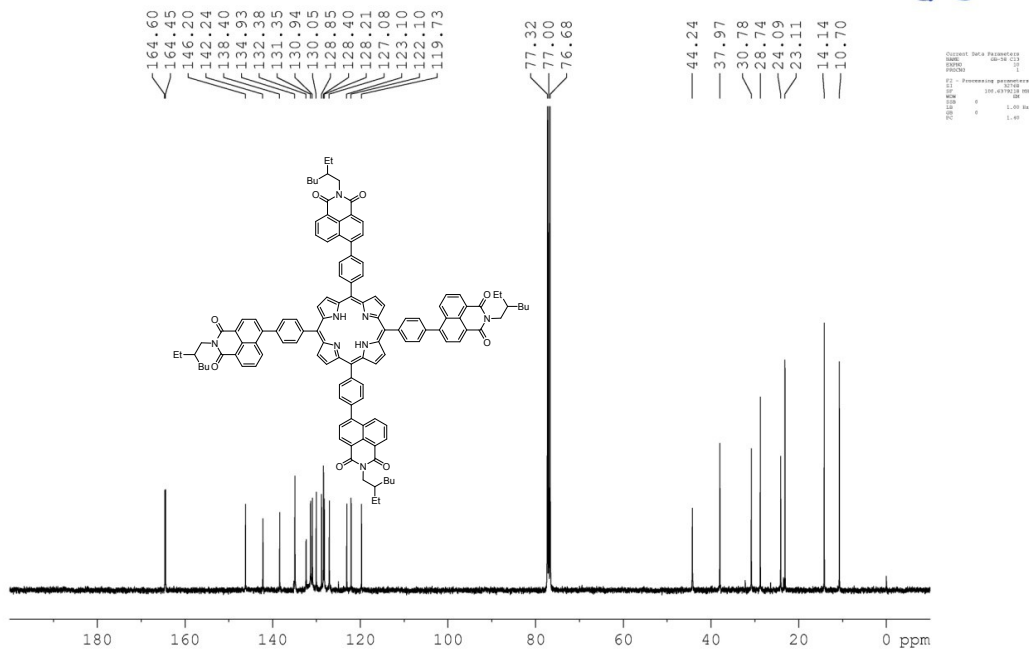


Figure S14. ^{13}C NMR spectra of $T(p\text{-NI})\text{PPH}2$ recorded in CDCl_3 .

HKBU_

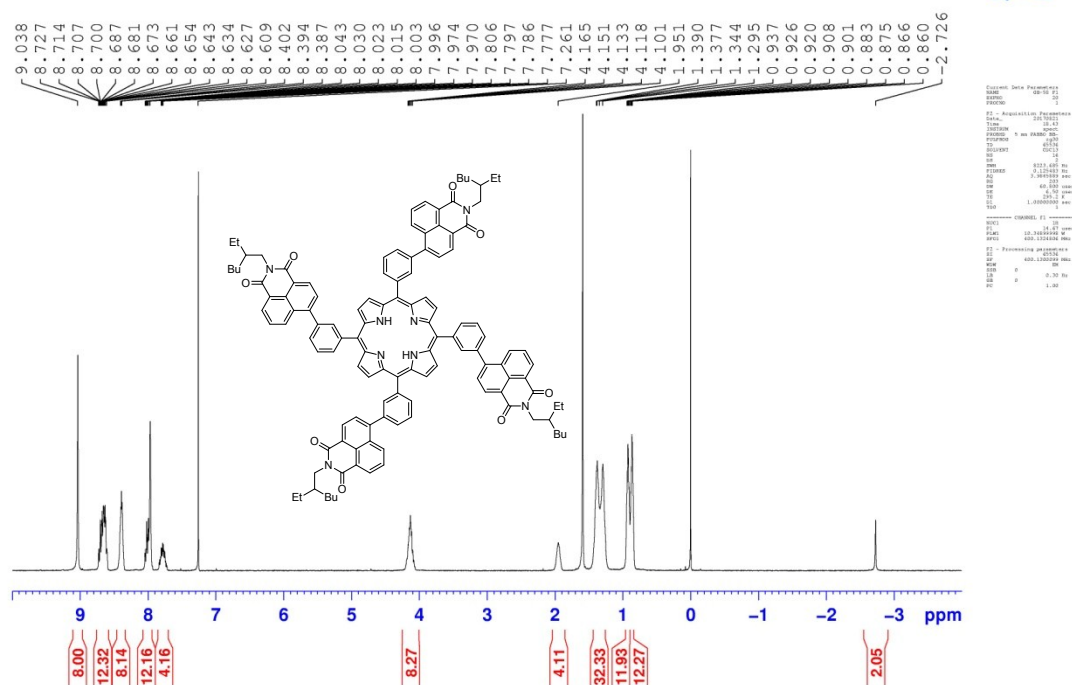
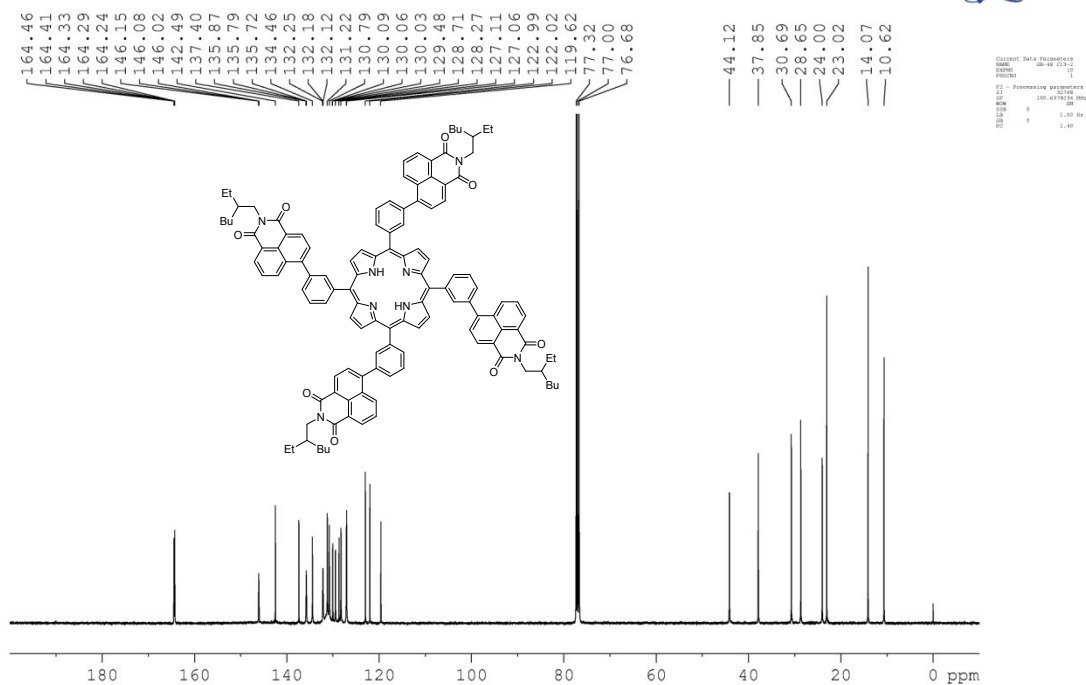
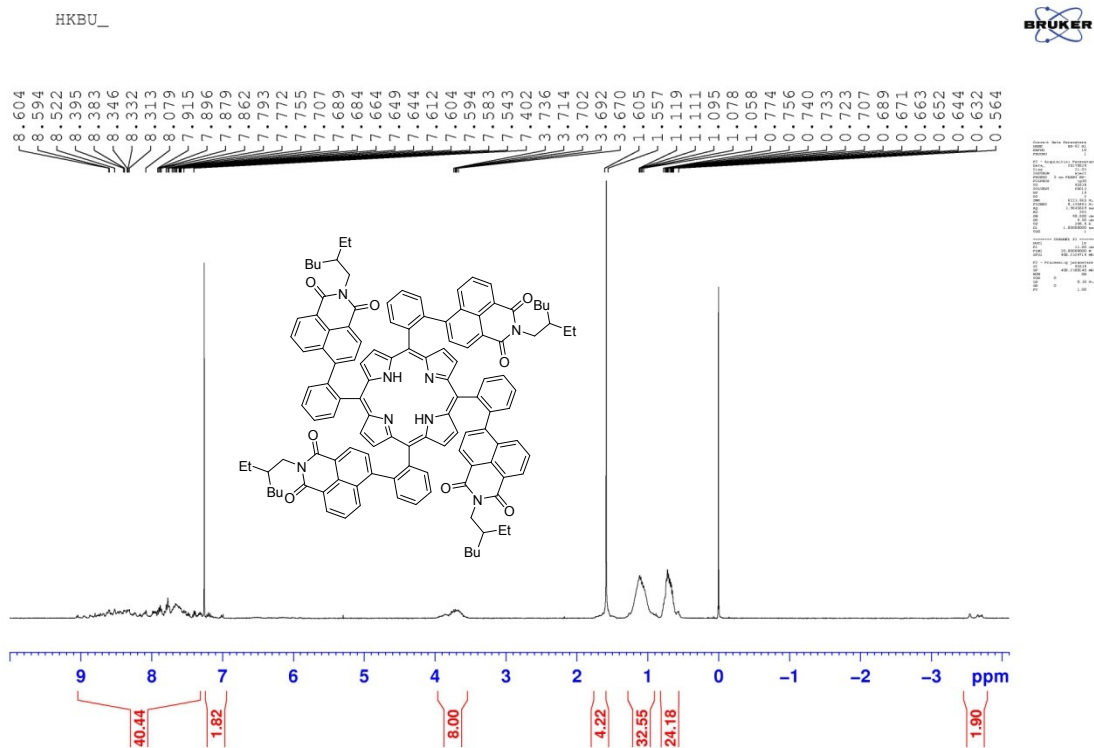


Figure S15. ^1H NMR spectra of $T(m\text{-NI})\text{PPH}2$ recorded in CDCl_3

Figure S16. ^{13}C NMR spectra of $\text{T}(m\text{-NI})\text{PPH}_2$ recorded in CDCl_3 .Figure S17. ^1H NMR spectra of $\text{T}(o\text{-NI})\text{PPH}_2$ recorded in CDCl_3 .

GB-62 C13

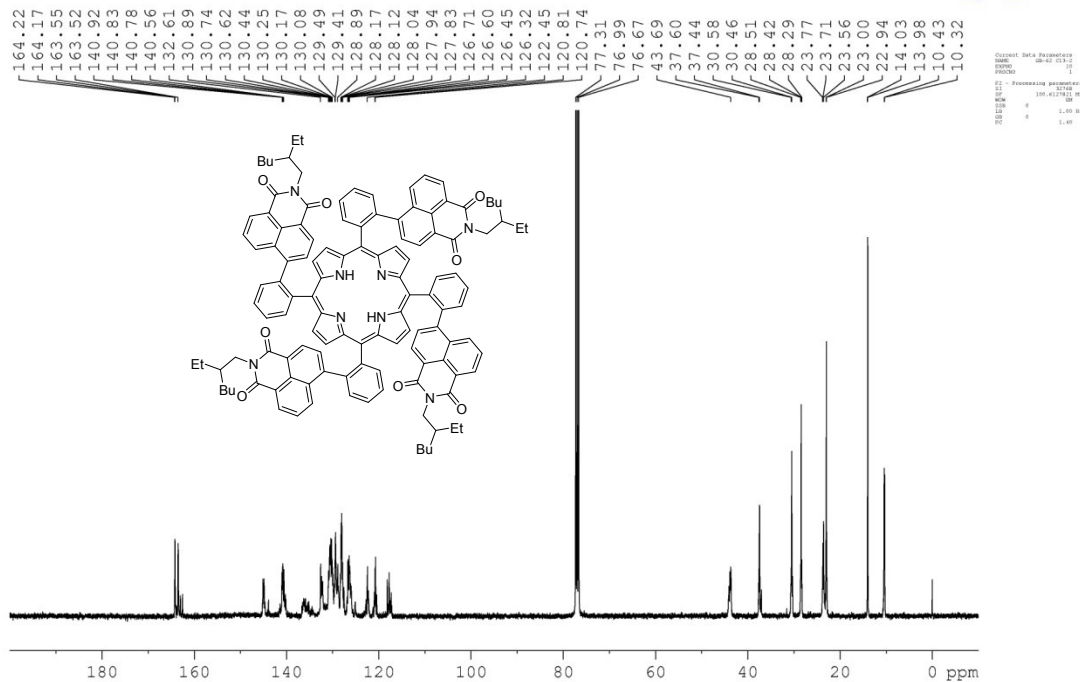


Figure S18. ¹³C NMR spectra of T(o-NI)PPH recorded in CDCl₃.

GB-49

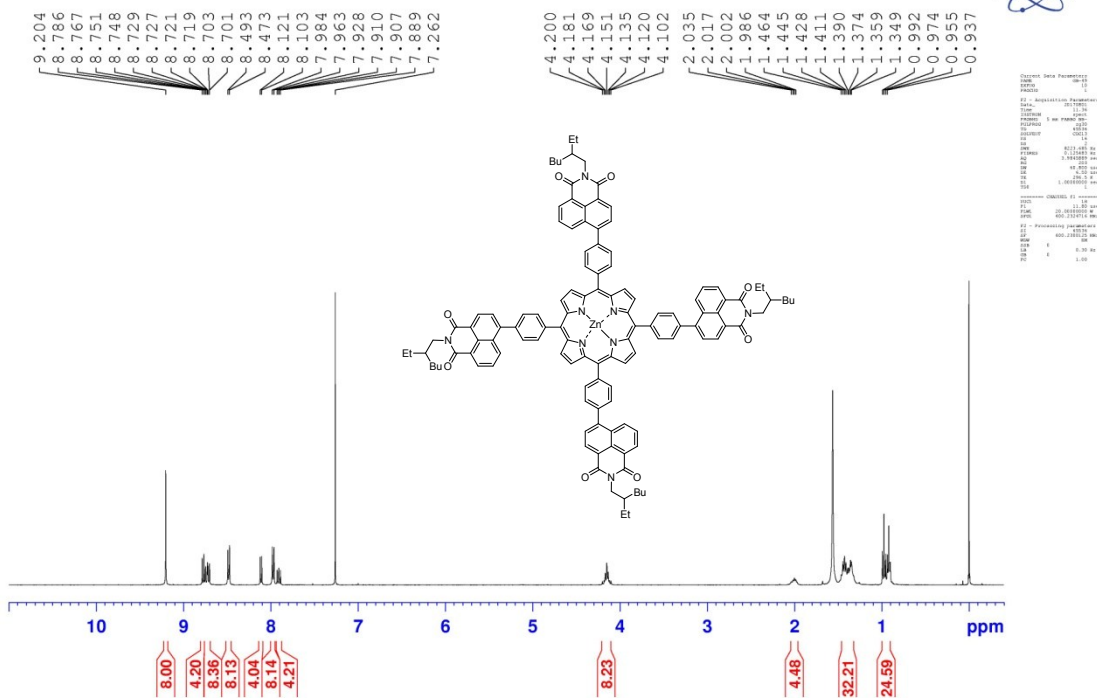


Figure S19. ¹H NMR spectra of ZnT(p-NI)PP recorded in CDCl₃.

GB-49 C13

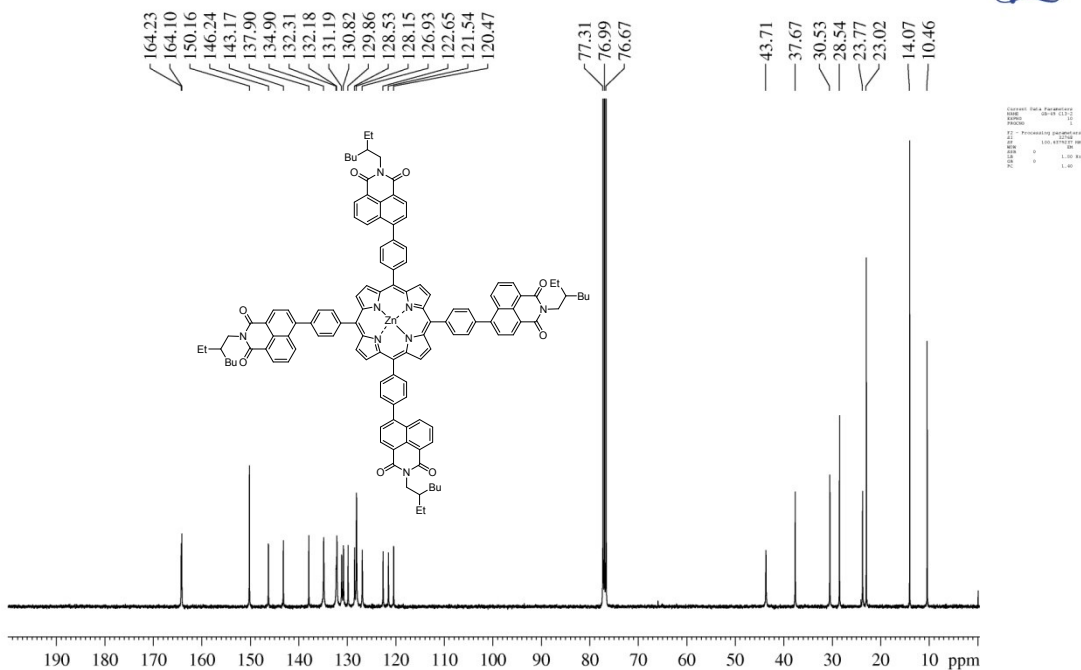


Figure S20. ^{13}C NMR spectra of ZnT(*p*-NI)PP recorded in CDCl_3 .

GB-60

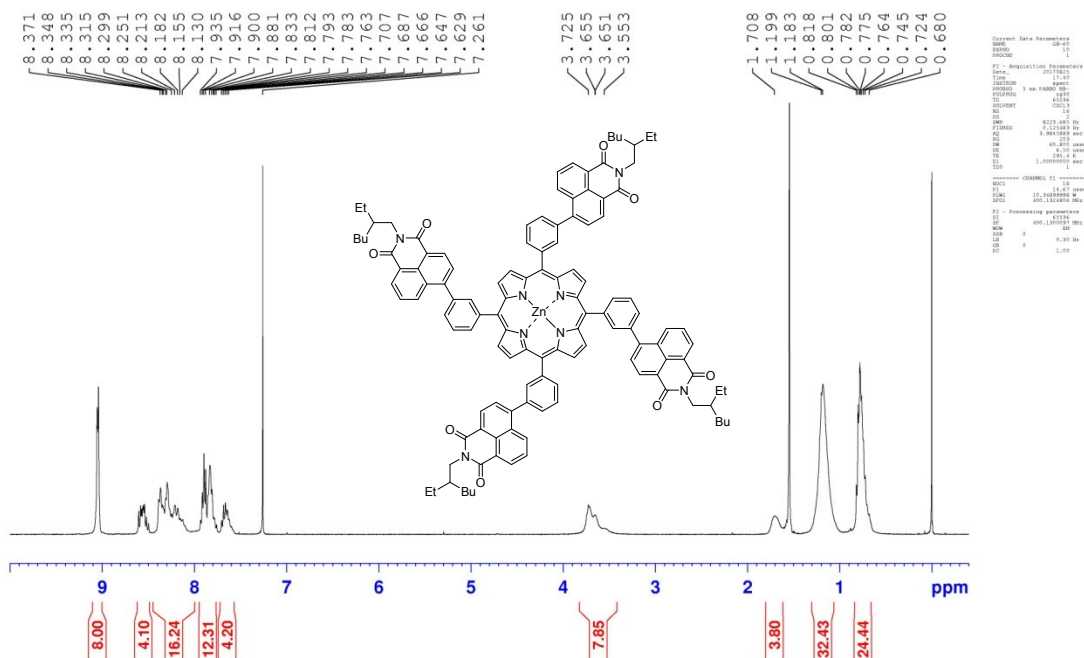
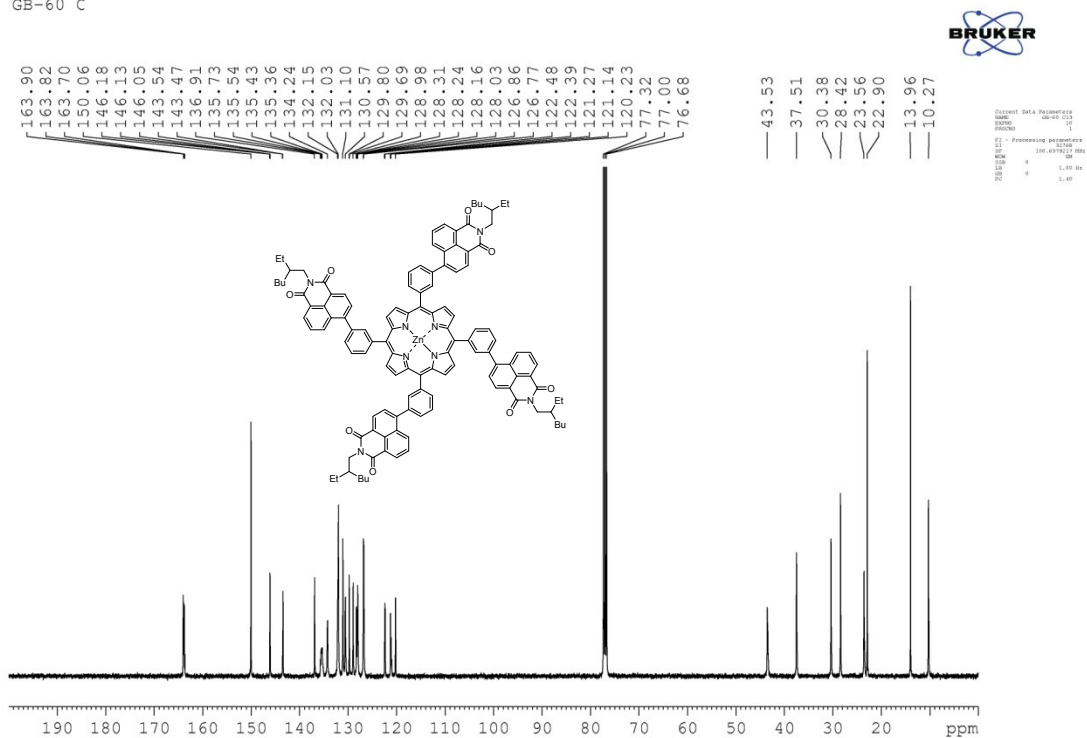
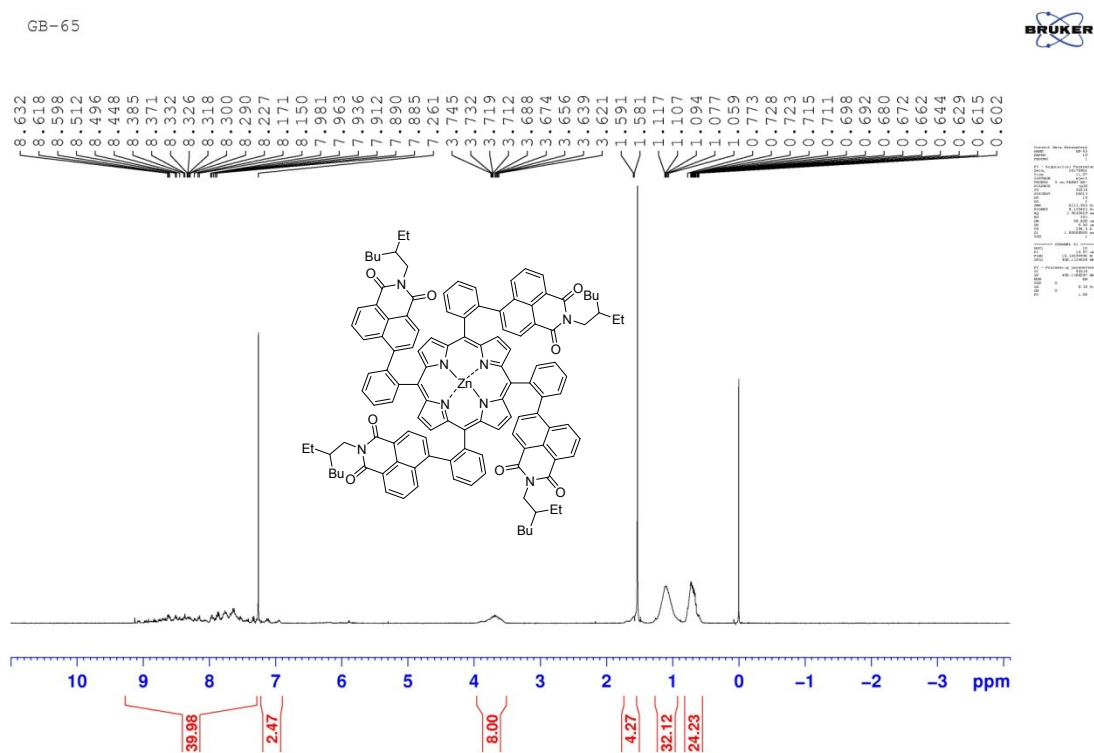


Figure S21. ^1H NMR spectra of ZnT(*m*-NI)PP recorded in CDCl_3 .

GB-60 C

Figure S22. ^{13}C NMR spectra of $\text{ZnT}(m\text{-NI})\text{PP}$ recorded in CDCl_3 .

GB-65

Figure S23. ^1H NMR spectra of $\text{ZnT}(o\text{-NI})\text{PP}$ recorded in CDCl_3 .

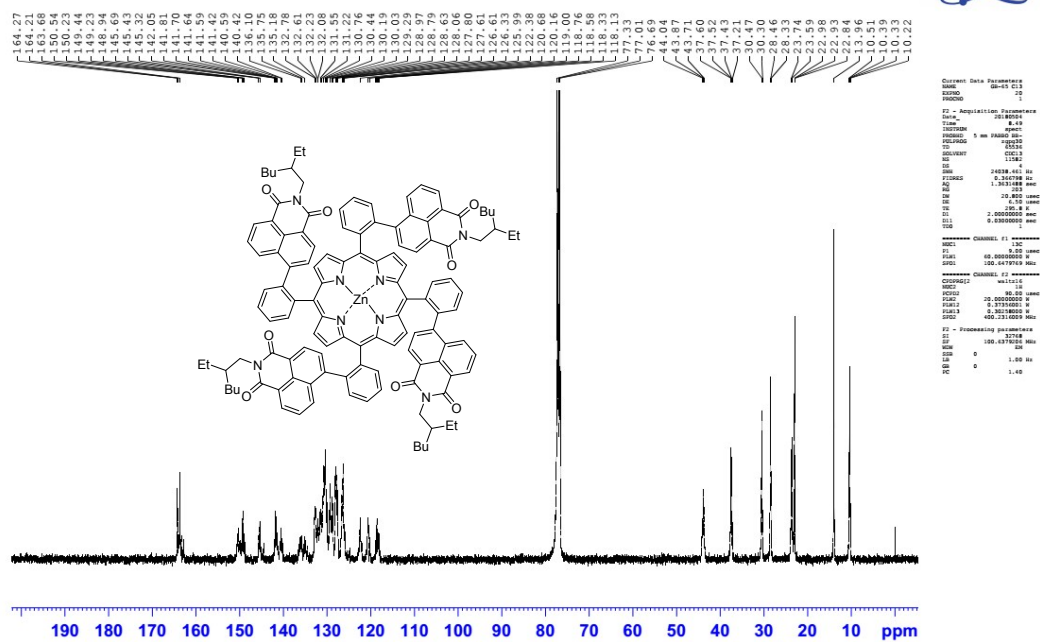


Figure S24. ^{13}C NMR spectra of $\text{ZnT}(o\text{-NI})\text{PP}$ recorded in CDCl_3 .

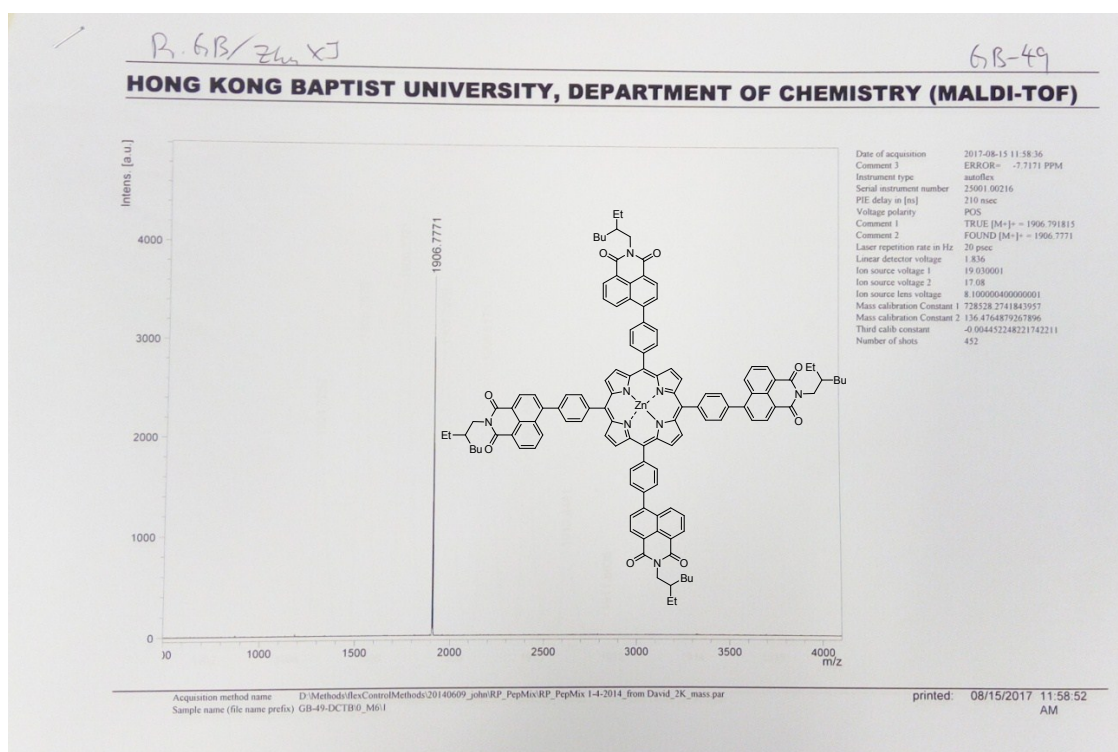


Figure S25. MALDI-TOF-MS spectra of $\text{ZnT}(p\text{-NI})\text{PP}$.

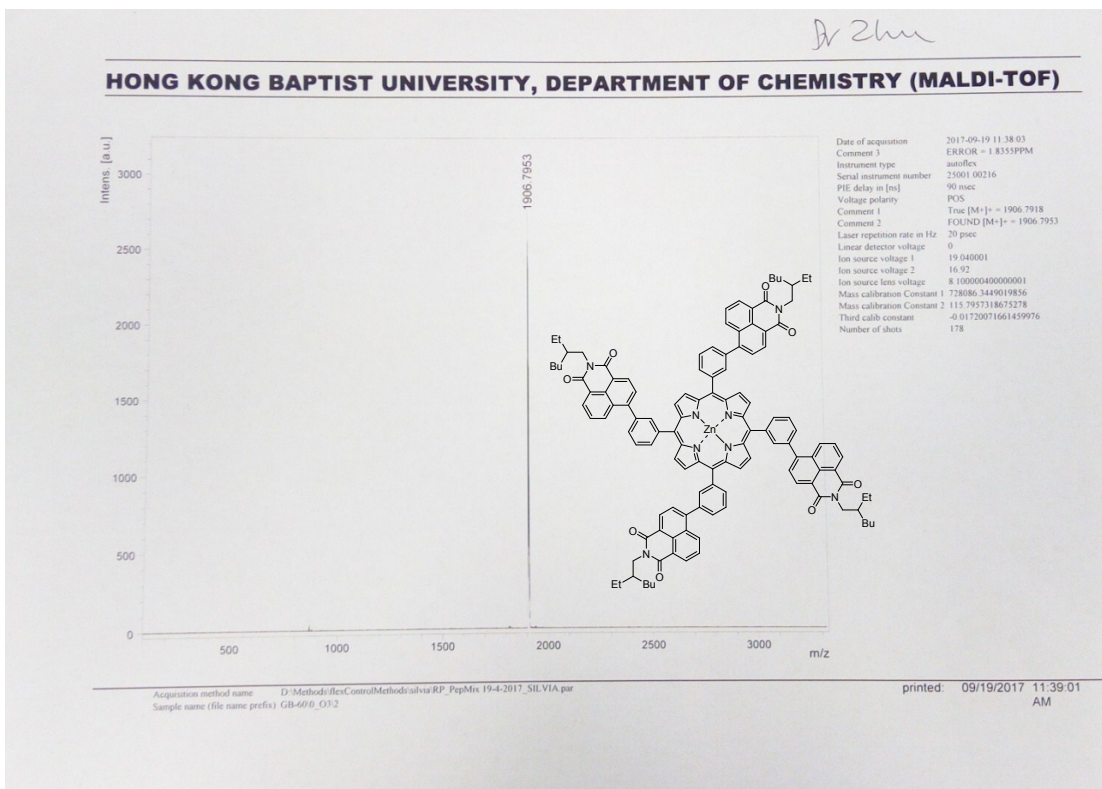


Figure S26. MALDI-TOF-MS spectra of **ZnT(*m*-NI)PP**.

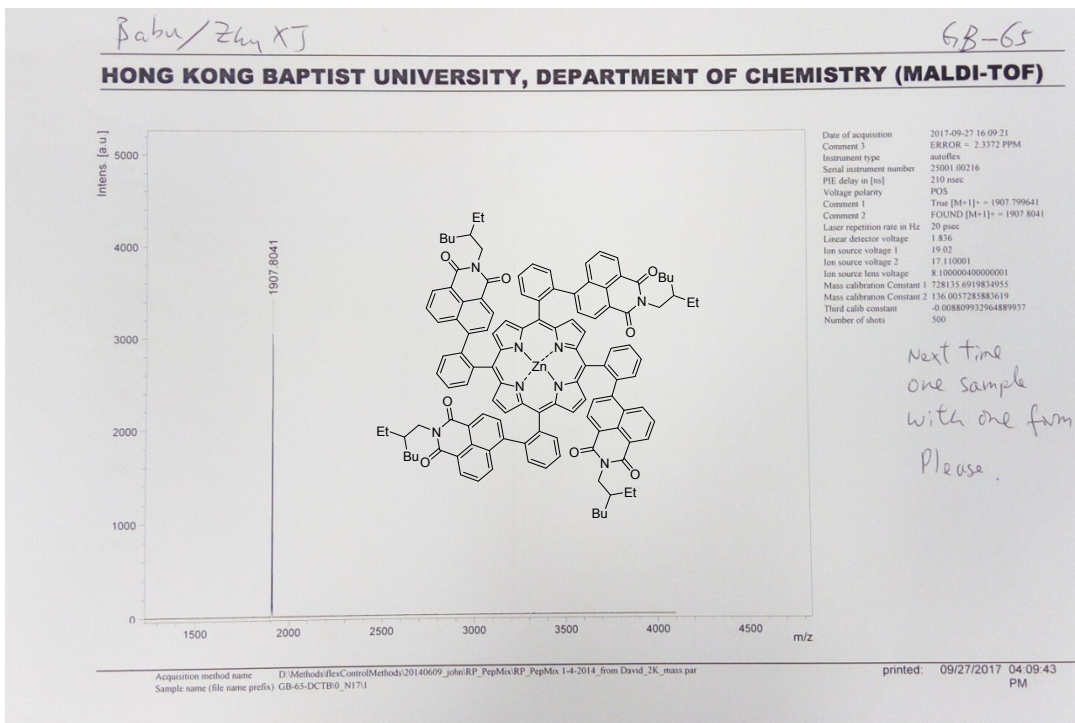


Figure S27. MALDI-TOF-MS spectra of **ZnT(*o*-NI)PP**.

References

1. M. A. Shawkat, E. C. JR, D. H. Pierre, Introduction to Photophysics and Photochemistry. In *Macromolecules Containing Metal and Metal-Like Elements*. <https://doi.org/10.1002/9780470604090.ch1>.
2. C. S. Sample, E. Goto, N. V. Handa, Z. A. Page, Y. Luo and C. J. Hawker, *Journal of Materials Chemistry C*, 2017, **5**, 1052-1056.
3. S. Erten-Ela, S. Ozcelik, and E. Eren, *Journal of Fluorescence*, 2011, **21**, 1565–1573.
4. T. T. H. Tran, G.-L. Chen, T. K. A. Hoang, M.-Y. Kuo and Y. O. Su, *The Journal of Physical Chemistry A*, 2017, **121**, 6925-6931.